Regeneration of Sensory Hair Cells and Restoration of Vestibular Function by Notch Inhibition

Hanae Lahlou[1,2], Hong Zhu[3], Wu Zhou[3] and Albert S.B. Edge[1,2,4*]

[1] Department of Otolaryngology, Harvard Medical School; Boston, MA, USA.
[2] Eaton-Peabody Laboratory, Massachusetts Eye and Ear; Boston, MA, USA.
[3] Department of Otolaryngology-Head and Neck Surgery, University of Mississippi Medical Center; Jackson, MS, USA.
[4] Harvard Stem Cell Institute; Cambridge, MA, USA.

*Corresponding author. Email: albert_edge@meei.harvard.edu

Abstract
Sensory hair cell loss in the vestibular organs of the inner ear causes balance disorders which are essentially irreversible due to the lack of significant hair cell regeneration. Here, we administered a γ-secretase inhibitor to an adult mouse model of vestibular hair cell loss. The treatment resulted in complete regeneration of type II and partial restoration of type I hair cells after one month and restored vestibuloocular reflexes across all frequencies of rotational and linear acceleration. Further recovery was apparent at 8 months. Genetic deletion of *Notch1* in supporting cells identified Notch1 as the target of the drug. The results demonstrate that a single injection of a γ-secretase inhibitor is a viable therapy for functional restoration of the vestibular system in patients with balance disorders.

Introduction

Loss of mechanoreceptor hair cells in the cochlear and vestibular organs of the inner ear causes disorders of hearing and balance. Hair cells are vulnerable to insults such as acoustic trauma and ototoxic agents, as well as mutations and damage due to aging (*1-4*). These exposures cause irreversible damage, because of the inability of the inner ear organs to regenerate physiologically active hair cells, and can be debilitating, comprising a top disability in individuals over age 70 (*1, 5*). Vestibular hair cells reside in the semicircular canals and otolith organs of the inner ear that sense angular and linear acceleration, respectively. Two types of vestibular sensory cells, type I and type II hair cells, are interdigitated by supporting cells in a sensory epithelium (*6*) and innervated by afferent neurons (*4, 7-9*) that encode head acceleration signals for transmission to the central nervous system.

While non-mammalian vertebrates display continuous vestibular cell turnover throughout life and can spontaneously regenerate hair cells in response to damage (*10-16*), the capacity of mammalian vestibular organs for regeneration declines after the early postnatal period (*10-23*). In newborn mammals, supporting cells appear to act as progenitors to regenerate type I and type II hair cells (*14, 23, 24*), which are thought to result from independent developmental trajectories from a common progenitor cell (*25*). The limited regeneration seen in the mature utricle (*11, 26*) leads exclusively to hair cells of type II phenotype. The failure to regenerate type I hair cells, along with the insufficient recovery of type II hair cells, impedes functional restoration, as both are vital for sensing head movement (*20, 23, 27-29*). Cellular reprogramming using pro-differentiation factors in the adult cochlea has resulted in limited hair cell regeneration from supporting cells and no functional recovery (*30-32*). Studies on recovery of balance have relied on the overexpression of bHLH transcription factor, Atoh1, to reprogram supporting cells to hair cells in mature vestibular organs but have not restored a high level of vestibular function (*20, 33*).

Here, we investigated the use of a γ-secretase inhibitor to stimulate vestibular hair cell regeneration in an adult mouse model of hair cell ablation. We show significant regeneration of type I and II hair cells, resulting in near-complete recovery of vestibular function across stimulus frequencies. The new hair cells were structurally integrated into the sensory epithelium and rescued canal and otolith organ function, restoring head rotation- and translation-evoked

vestibuloocular reflexes (VORs). Treatment with a γ-secretase inhibitor thus represents a potential therapeutic approach to this important and widespread disability.

Results

Hair cell regeneration induced by γ-secretase inhibitor, LY411575, in *Pou4f3*^{DTR} -ablated utricle and canal cristae

We chose to test a γ-secretase inhibitor to treat hair cell loss in the adult utricle. These drugs are effective tools for conversion of inner ear supporting cells to hair cells in newborn cochlear and vestibular organs (*34-36*) and in cochlear organoids (*37*). Although their effect is limited in the adult cochlea (*30, 38, 39*), we chose to test the effect of γ-secretase inhibitors in the vestibular system because it retains some regenerative capacity into adulthood (*40*).

We administered γ-secretase inhibitor, LY411575 (LY), by unilateral injection onto the round window membrane of DT-ablated *Pou4f3*$^{DTR/+}$ mice (*11*), 7 days after hair cell ablation (Fig. 1A). In these mice, the *Pou4f3* promoter drives expression of the human diphtheria toxin receptor (DTR) in hair cells, and administration of DT results in near-complete ablation of hair cells. Following ablation, vestibular epithelia were immunostained for SRY-box transcription factor 2 (Sox2), myosin7a (Myo7a) and tenascin (Tnc) to identify supporting cells (Myo7a-Sox2+), and type I (Myo7a+Tnc+) and type II (Myo7a+Sox2+) hair cells (Fig. 1B).

Examination of the anterior, posterior, and horizontal semicircular canals one month after LY treatment revealed an increase in type I and type II hair cells after drug treatment (Fig. 1C). The increase in hair number was accompanied by an increase in the number of supporting cells in the LY-treated cristae compared to untreated controls where regeneration occurred spontaneously (Fig. 1D).

Analysis of the utricle showed abundant Myo7a+ cells in both untreated (-LY) and drug-treated (+LY) ears after one month (Fig. 1E). However, while spontaneous regeneration in the adult mouse utricle was limited to type II hair cells as expected *(10, 13, 18)*, regeneration after LY treatment comprised type I and type II cells. These cells were apparent in both striolar and extrastriolar regions of the utricle (Fig. 1F and G). Quantification also showed a greater number of supporting cells (Myo7a-Sox2+) in the DT-damaged utricle treated with LY, compared to untreated controls (Fig. 1G).

Increased hair cell regeneration in *Pou4f3*$^{DTR/+}$-ablated utricle by *Notch1* knockout in supporting cells

Treatment with a γ-secretase inhibitor was chosen as the therapeutic approach because of the known effect of inhibiting this enzyme on signaling pathways important for maintaining hair cell identity (*34, 36, 38*). However there are more than 90 known γ-secretase substrates (*41*), and we sought to identify the substrate most important for these effects on the vestibular system. One γ-secretase-affected pathway is Notch signaling, which guides the fate distinction between hair cells and supporting cells during development (*35, 42*), and which has been shown to influence hair cell regeneration in the newborn inner ear. To investigate whether *Notch1* was the target for

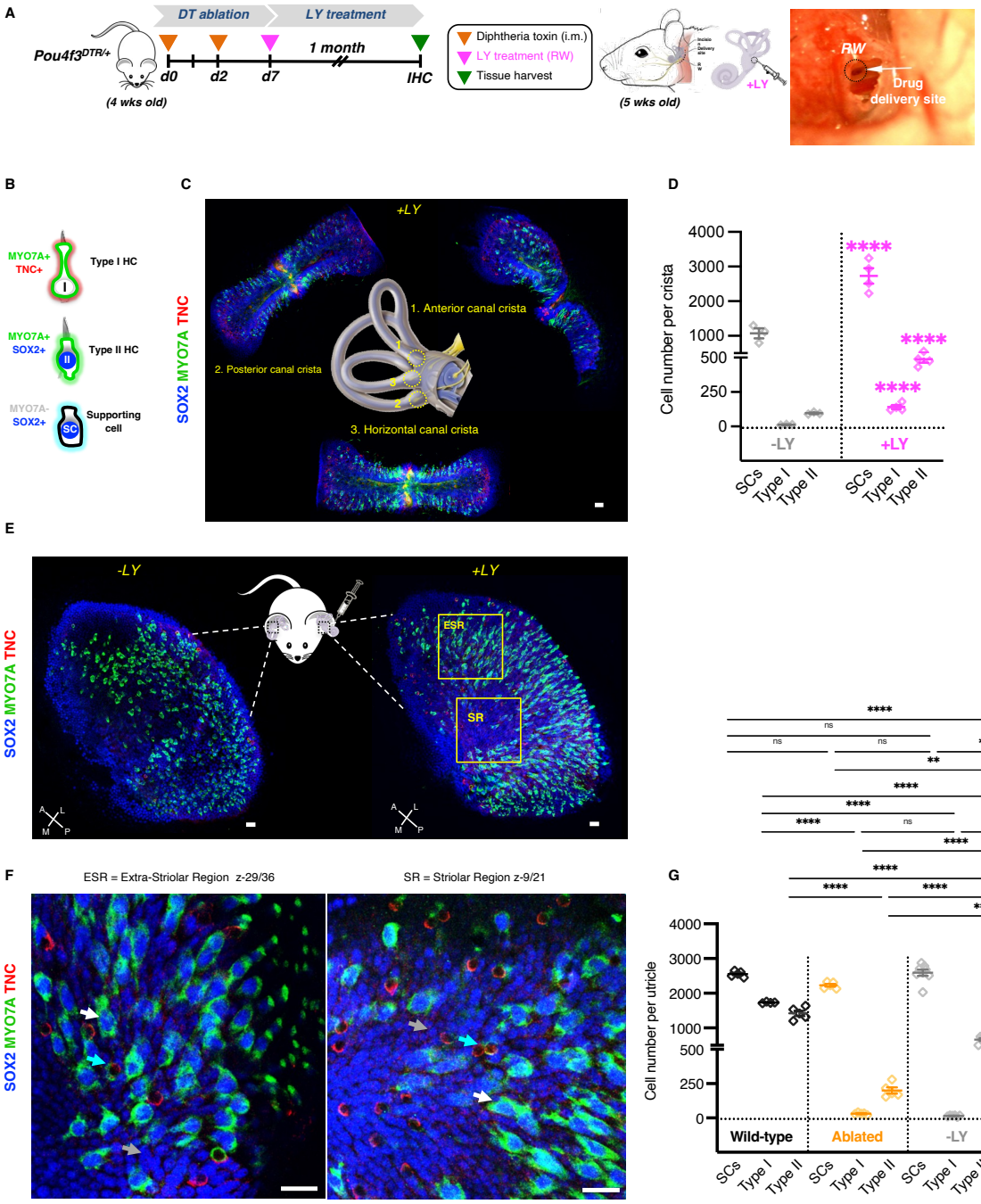

Fig. 1. LY treatment promotes type I and type II hair cell regeneration in the vestibular organs. (A) Schematic of the *in vivo* approach for drug delivery in DT-pretreated *Pou4f3*$^{DTR/+}$ mice. LY was injected in the left ear via the round window at day 7 post DT damage; the contralateral ear was used as a control for spontaneous regeneration. Mice were examined 1 month after drug treatment. **(B)** Diagram of type I (Myo7a+Tnc+) and type II (Myo7a+Sox2+) hair cells and supporting cells (Myo7a-Sox2+). **(C)** Immunolabeled cristae from drug treated ear. **(D)** Quantification of supporting cells, type I and type II hair cells from cristae of untreated (-LY) and treated (+LY) ears. **(E)** Sox2 (blue), Myo7a (green) and Tnc (red) immunolabelled utricles from untreated (-LY) and treated (+LY) ears. **(F)** High-magnification images from the striolar and extrastriolar regions indicating the presence of supporting cells (gray arrows), type I hair cells (cyan arrows) and type II hair cells (white arrows). **(G)** Quantification of supporting cells, type I and type II hair cells from wild-type, DT-ablated, untreated (-LY) and treated (+LY) utricles. All data represent the mean ± SEM. ****$p < 0.0001$, ***$p < 0.001$, **$p < 0.01$ by 1-way ANOVA with Tukey's multiple comparisons test. Scale bars = 50 - 100 µm.

the effect of the γ-secretase inhibitor on vestibular hair cell regeneration, we conditionally knocked out *Notch1* (*Notch1*^{cKO}) in supporting cells of the *Pou4f3*$^{DTR/+}$ mouse crossed to a *Plp1*^{CreER} mouse to activate the expression of *tdTomato* 7 days prior to DT-mediated ablation of hair cells. DT was administered at days 0 and day 2 of the experiment to 4-week-old *Pou4f3*$^{DTR/+}$ heterozygous mice (Fig. 2A). As *Plp1* expression is restricted to supporting cells in the utricular sensory epithelium (*43*), our lineage tracing approach followed *tdTomato* cells exhibiting red fluorescence upon Cre activation.

At one month, *Notch1* knockout resulted in robust Myo7a+ hair cell regeneration (Fig. 2B). Immunostaining showed that new hair cells in the lineage-traced mice were derived from *Plp1tdTom*+ supporting cells and differentiated into both type I (Myo7a+Tnc+) and type II (Myo7a+Sox2+) hair cells. Tnc staining confirmed the presence of calyces surrounding the base of the type I cells which were further identified through orthogonal views capturing the lineage tag in both type I and type II cells (Fig. 2C). Quantification indicated an increase in the number of both hair cell types in the *Notch1*^{cKO} ears, as well as an increase in supporting cell number (Fig 2F). Immunostaining showed that hair cells expressed espin in distinct stereociliary bundles (Fig. 2D), short and thin stereocilia characteristic of type II cells and longer, thicker stereocilia characteristic of type I cells (*6, 28, 44*). Regenerated hair cells were innervated (Fig. 2E) as shown by TuJ1 staining (Myo7a+tdTom+). The presence of stereocilia and innervation suggested a mature hair cell phenotype.

Two months after ablation (Fig. 2G), *Notch1* knockout resulted in a substantial increase in type I hair cells compared to 1 month (Fig. 2H). This increase was primarily due to regenerated *Plp1tdTom*+ cells (3% at 1 month *vs* 7% at 2 months) while the proportion of *Plp1tdTom*- type I cells remained the same (8%) (Fig 2I). Since the *Plp1* promoter is inactive in supporting cells within the striolar region (*18*), the type I cells arose from a distinct population of supporting cells that did not express *Plp1*. Notably, in orthogonal views (Fig. 2C), some type I hair cells were Sox2+, indicating that this population may represent Sox2+ supporting cells that contribute to type I hair cell regeneration in the striolar region.

Restoration of canal and otolith function by γ-secretase inhibition or *Notch1* knockout in supporting cells

To evaluate the impact of LY and *Notch1* knockout on vestibular recovery following hair cell regeneration, we assessed both canal and otolith function, which allow gaze stabilization in response to head rotation and translation at 2 months (Fig. 3A) and 8 months (Fig. 4A). Canal function was measured by the rotational vestibuloocular reflex (RVOR), and otolith via the translational vestibuloocular reflex (TVOR). RVOR was assessed both with and without visual stimulation to distinguish true vestibular recovery from any potential visual-vestibular interaction or central compensation, which is crucial for accurately interpreting functional restoration in the vestibular system.

Acute recovery of RVOR and TVOR

Consistent with the near-complete hair cell loss, both RVOR and TVOR gains were absent

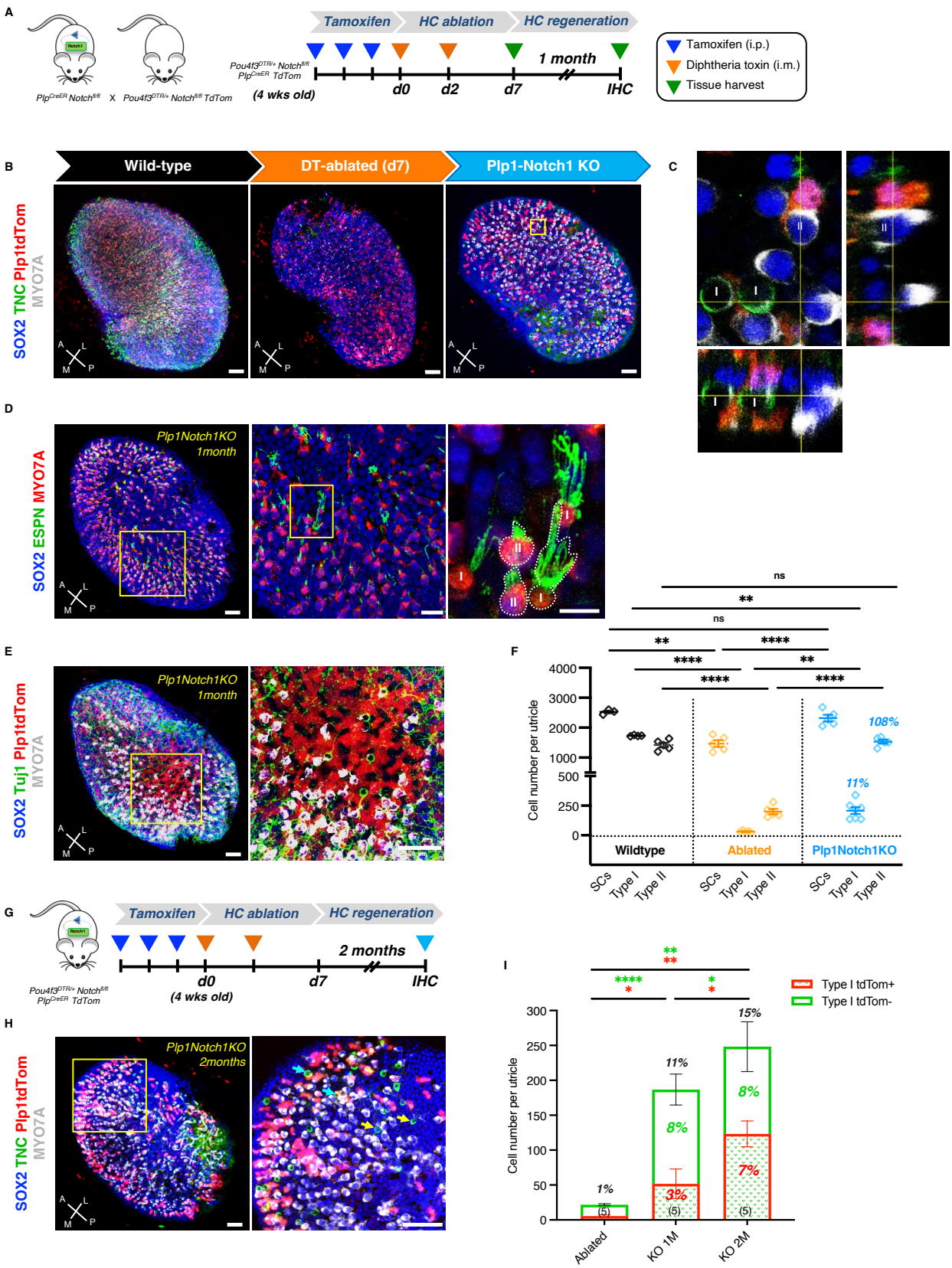
A
Tamoxifen
HC ablation
HC regeneration
1 month
d0
d2
d7
IHC
(4 wks old)
Tamoxifen (i.p.)
Diphtheria toxin (i.m.)
Tissue harvest
B
Wild-type
DT-ablated (d7)
Plp1-Notch1 KO
SOX2 TNC Plp1tdTom
MYO7A
C
D
Plp1Notch1KO
1month
SOX2 ESPN MYO7A
E
SOX2 Tuj1 Plp1tdTom
MYO7A
F
Cell number per utricle
Wildtype
Ablated
Plp1Notch1KO
SCs
Type I
Type II
108%
11%
ns
**
****
G
Tamoxifen
HC ablation
HC regeneration
2 months
d0
d7
IHC
(4 wks old)
H
Plp1Notch1KO
2months
SOX2 TNC Plp1tdTom
MYO7A
I
Type I tdTom+
Type I tdTom-
Cell number per utricle
Ablated
KO 1M
KO 2M
1%
11%
15%
8%
3%
7%
(5)

Fig. 2. Conditional knockout of *Notch1* in Plp1+ supporting cells increases type I and II hair cell regeneration in DT-ablated *Pou4f3*$^{DTR/+}$ mice. (A) Schematic of the experimental approach, *Pou4f3*$^{DTR/+}$ *Plp1*^{CreER} *Notch1*$^{fl/fl}$ *tdTom* and wild-type were subjected to tamoxifen to induce Cre-mediated recombination in *Plp1*^{CreER} *floxed-Notch1* followed by diphtheria toxin (DT) to ablate hair cells. (**B)** Utricles immunolabeled for Sox2 (blue), Tnc (green), Myo7a (green), with tdTomato (red) for fate mapping of supporting cells. (**C)** High magnification with an orthogonal view showing newly regenerated type I (Myo7a+Tnc+) and type II ((Myo7a+Tnc-Sox2+) hair cells arising from Plp1tdTom+ supporting cells. (**D)** *Pou4f3*$^{DTR/+}$ *Plp1*^{CreER} *Notch1*$^{fl/fl}$ DT-ablated utricle immunolabeled at 1 month for Sox2 (blue), Espn (green), Myo7a (red), high magnification images indicate the presence of stereociliary bundles in type I and type II hair cells. (**E)** *Pou4f3*$^{DTR/+}$ *Plp1*^{CreER} *Notch1*$^{fl/fl}$ *tdTom* DT-ablated utricle immunolabeled at 1 month for Sox2 (blue), Tnc (green), Myo7a (gray), with high magnification image showing innervation of type I (Myo7a+TNC+) and type II (Myo7a+Sox2+) hair cells. (**F)** Quantification of type I and type II hair cells and supporting cells. (**G)** Schematic of the experimental design for *Notch1*^{cKO} 2 months post DT-ablation. (**H)** *Pou4f3*$^{DTR/+}$ *Plp1*^{CreER} *Notch1*$^{fl/fl}$ *TdTom* DT-ablated utricle immunolabeled at 2 months for Sox2 (blue), Tnc (green), Myo7a (gray) with tdTomato (red) for fate mapping of supporting cells. High magnification image indicates type I cells arising from Plp1tdTom+ (cyan arrows) and Plp1tdTom- (yellow arrows). (**I**) Type I hair cell numbers from DT-ablated *Pou4f3*$^{DTR/+}$compared to *Pou4f3*$^{DTR/+}$ *Plp1*^{CreER} *Notch1*$^{fl/fl}$ *TdTom* mice 1 and 2 months after treatment. All data represent the mean ± SEM. ****$p < 0.0001$, **$p < 0.01$, *$p < 0.05$ by mixed effect model, repeated measures 2-way ANOVA with Tukey's post-hoc test. Scale bars = 50 - 100 µm.

in the DT-ablated mice (shown in gray lines) across all frequencies (Fig. 3B and E). Phase responses were highly variable (Fig. 3C', D' and F'), indicating a loss of the regular vestibular reflex needed for gaze stabilization. Additionally, notable distortion was observed in the residual responses, reflecting disrupted vestibular function (Fig. 3C", D" and F').

Two months after γ-secretase inhibitor treatment (pink lines), the increase in hair cells led to a significant restoration of the RVOR gain across all frequencies (Fig. 3C-D), with phase (Fig. C'-D') responses approaching wild-type levels and with low distortion (Fig. 3C"-D"), indicating a recovery of canal function to near-normal. *Notch1*^{cKO} mice (blue lines) also showed improvements in RVOR gain and phase, though the extent of recovery was less than for LY treatment (Fig. 3G).

Both LY-treated and *Notch1*^{cKO} mice (pink vs. blue lines) exhibited compensatory gains in TVOR (Fig. 3F) at 2 Hz and phases (Fig. 3F') that were comparable to wild-type levels (Fig. 3G). Improved phase responses with minimal distortion (Fig. 3F"), suggested effective compensation. No significant differences were observed between the two treatments, indicating that each approach effectively restored TVOR function to a similar extent (Fig. 3G).

Long-term effects on RVOR and TVOR

We next assessed the effect of γ-secretase treatment and *Notch1* knockout at later time points to evaluate the impact of hair cell regeneration on vestibular recovery and stability. While the DT-ablated mice without treatment (gray lines) showed persistent deficits in both RVOR and TVOR gain across all frequencies 8 months after hair cell ablation, indicating no spontaneous recovery of vestibular function, the LY-treated (pink lines) and *Notch1*^{cKO} (blue lines) groups demonstrated significant improvements in VOR responses (Fig. 4B-D). γ-secretase inhibition and *Notch1*^{cKO} resulted in a substantial increase in RVOR gains, with or without visual stimulation (Fig. 4B and C). Both groups exhibited normal RVOR responses across all frequencies, with values

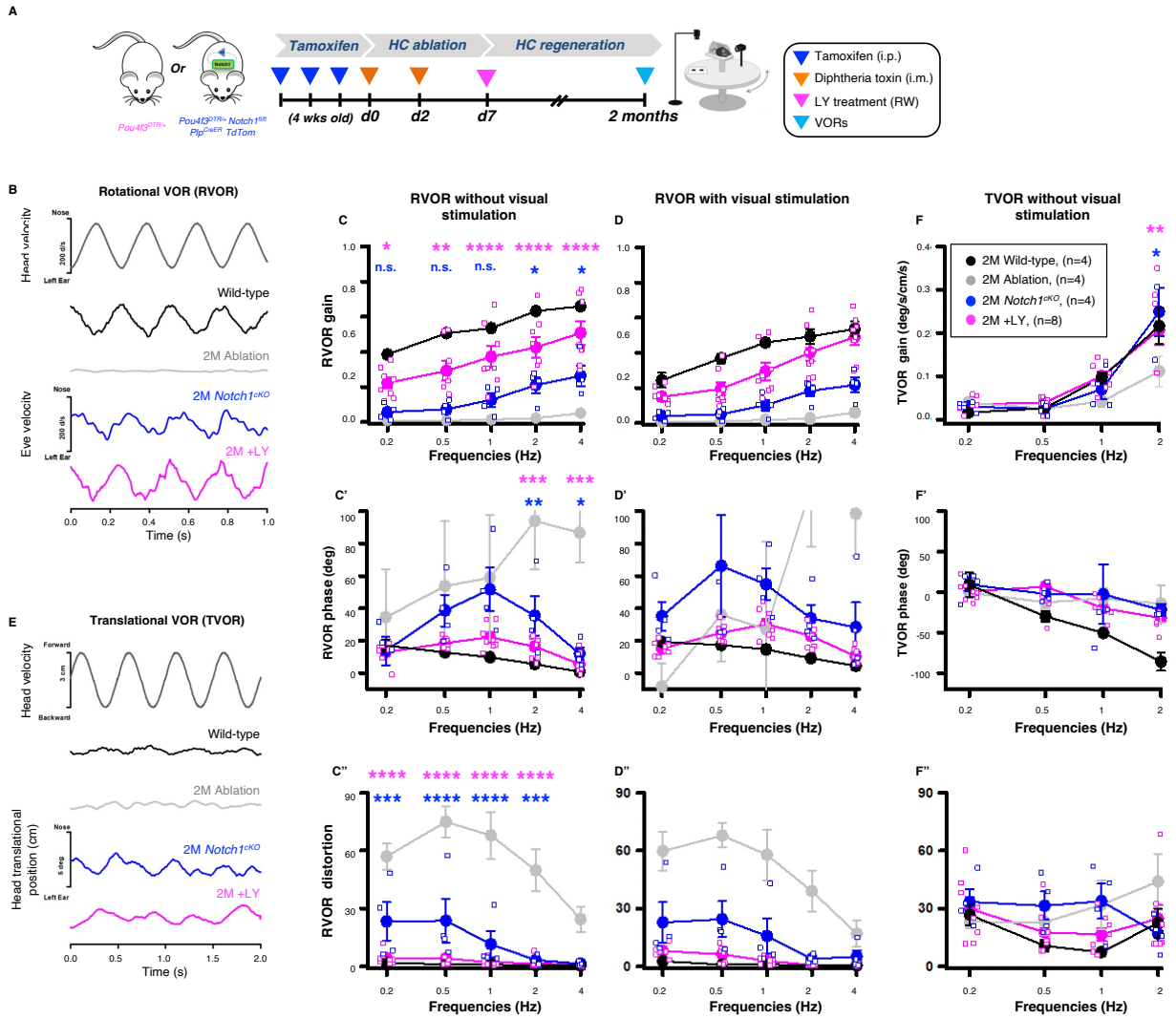

G

		N	P-values (2-way ANOVA with Tukey multiple comparisons) 0.2 Hz	0.5 Hz	1 Hz	2 Hz	4 Hz
RVOR gains	2M Wildtype vs. 2M *Notch1*^{cKO}	(4, 4)	*0.0102	****<0.0001	****<0.0001	****<0.0001	****<0.0001
	2M Wildtype vs. 2M +LY	(4, 8)	0.245	*0.011	*0.0176	0.274	0.704
	2M +LY vs. *Notch1*^{cKO}	4, 8)	0.159	*0.045	**0.0048	**0.001	****<0.0001
TVOR gains	2M Wildtype vs. 2M *Notch1*^{cKO}	(4, 4)	0.927	0.998	0.755	0.658	
	2M Wildtype vs. 2M +LY	(4, 8)	0.830	0.916	0.995	0.959	
	2M +LY vs. *Notch1*^{cKO}	4, 8)	0.987	0.890	0.631	0.409	

Fig. 3. Recovery of ROVR and TVOR following a single dose of LY or *Notch1* knockout at 2 months post DT-ablation. (A) Schematic of the experimental approach of tamoxifen administration to induce Cre-mediated recombination in *Plp1*^{CreER} *Notch1*$^{fl/fl}$ followed by DT to ablate hair cells. Rotational and translational VORs were recorded from wild-type (n=4), *Pou4f3*$^{DTR/+}$ DT-ablated without any treatment (n=4), *Pou4f3*$^{DTR/+}$ DT-ablated +LY (n=8) and *Pou4f3*$^{DTR/+}$ DT-ablated *Notch1*^{cKO} mice (n=4). **(B)** Rotational vestibuloocular reflexes (rVORs) to sinusoidal head rotations with representative eye velocity responses to 4 Hz head rotation at 2 months post ablation, from wild-type (black), 2 months ablation (gray), +LY treatment (pink) and *Notch1*^{cKO} mice (blue). **(C)** RVOR gains without visual stimulation **(C)** with visual stimulation **(D).** RVOR phases without visual stimulation **(C')** with visual stimulation **(D').** RVOR distortions without visual stimulation **(C")** with visual stimulation **(D"). (E)**. Translational

vestibuloocular reflexes (TVORs) in response to sinusoidal head translation at 2 Hz 2 months post ablation, from wild-type (black), 2 months ablation (gray), +LY treatment (pink) and *Notch1*^{cKO} mice (blue). **(F)** TVOR gains. **(F')** TVOR phases. **(F")** TVOR distortion. All data represent the mean ± SEM. ****$p < 0.0001$, ***$p < 0.001$, **$p < 0.01$ **$p < 0.01$, *$p < 0.05$ by 2-way ANOVA with Tukey's multiple comparisons; p-values reported in the graphics are from the comparisons of LY and *Notch1*^{cKO} to the spontaneous regeneration 2 months post ablation. **(G)** Summary table of p-values comparing RVOR and TVOR gains from LY, *Notch1*^{cKO} and wild-type groups.

approaching the wild-type level (Fig. 4E). Phase (Fig. 4B'-C') and distortion (Fig. 4B"-C") measurements showed improved synchronization between head motion and eye movement.

RVOR gain in the 8-month *Notch1*^{cKO} mice improved significantly compared to 2 months, with stabilized phase responses and reduced distortion, suggesting improved vestibular compensation and successful integration of regenerated hair cells into vestibular circuits. However, the extent of recovery in the 8-month LY-treated group was more pronounced at high frequency compared to *Notch1*^{cKO} (Fig. 4E). This pattern was also observed in phase and distortion measurements, where LY treatment promoted more synchronized head motion and eye movement.

At 8 months, both LY-treated and *Notch1*^{cKO} mice exhibited TVOR gains statistically equivalent to wild-type (Fig. 4E). The improvement in TVOR gain was stable across all tested frequencies, suggesting effective long-term compensation. Although both treatments showed TVOR gains (Fig. 4D), LY-treated animals maintained a more synchronized phase response (Fig. 4D') and reduced distortion (Fig. 4D"), indicating a more complete recovery of vestibular function.

These results demonstrate that both γ-secretase inhibition and *Notch1* knockout drive hair cell regeneration and recovery of canal (RVOR) and otolith (TVOR) function. The recovery across frequencies is consistent with the observed regeneration of type I and type II hair cells in the canal and otolith organs. The greater high frequency improvement and more consistent long-term efficacy of the LY treatment compared to *Notch1* knockout suggests that the γ-secretase inhibitor is a more promising approach for restoring vestibular function than *Notch1* gene manipulation.

Discussion

A lack of treatments to achieve reversal is a persistent problem for balance disorders (*5*). We demonstrate here that inhibition of γ-secretase inhibitor, LY, one week after ablation resulted in regeneration of hair cells in mouse utricle at 1 month, partially replacing type I hair cells and replacing all type II hair cells. The regeneration of hair cells resulted in a near-complete restoration of vestibular function across test-frequencies. This represents a clear advantage over previously achieved regeneration with a GSK3β inhibitor (*45*).

The genetic deletion of *Notch1* resulted in quantitatively indistinguishable hair cell regeneration and functional improvement as the treatment with a γ-secretase inhibitor at 2 months after treatment. This allowed further analysis of the signaling in the conversion of supporting cells to hair cells and indicated that *Notch1* was likely the target accounting for the profound effect of the γ-secretase inhibitor, an important point because of the large number of possible γ-secretase substrates (*41*).

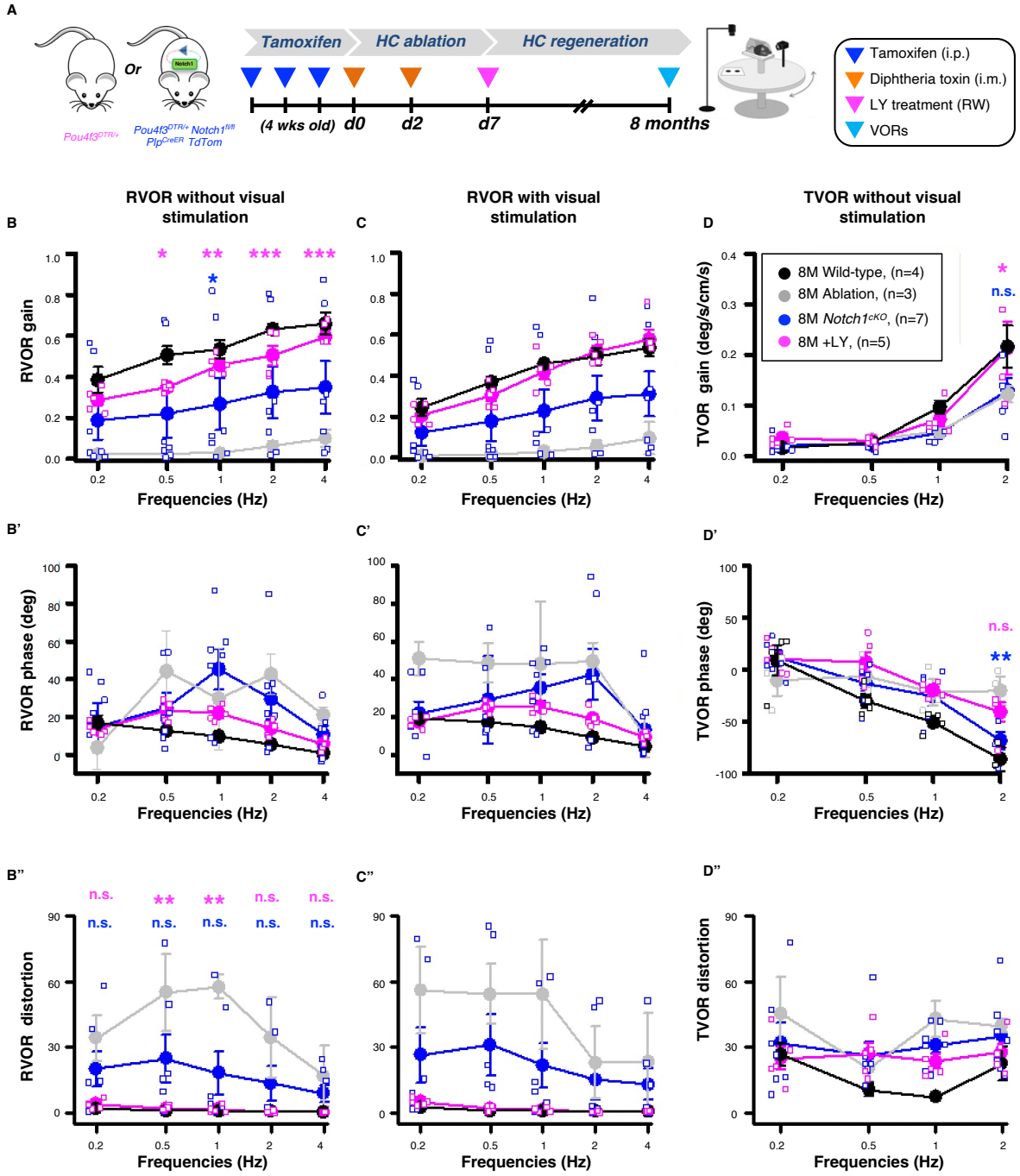

E

		N	P-values (2-way ANOVA with Tukey's multiple comparisons) 0.2 Hz	0.5 Hz	1 Hz	2 Hz	4 Hz
RVOR gains	8M Wild-type *vs.* 8M *Notch1*^{cKO}	*(4, 7)*	0.542	0.228	0.228	0.193	0.1314
	8M Wild-type *vs.* 8M +LY	*(4, 5)*	0.952	0.854	0.854	0.976	0.9435
	8M +LY *vs.* 8M *Notch1*^{cKO}	*(5, 7)*	0.710	0.479	0.479	0.093	*0.0425
TVOR gains	8M Wild-type *vs.* 8M *Notch1*^{cKO}	*(4, 7)*	0.983	0.989	0.186	*0.0113	
	8M Wild-type *vs.* 8M +LY	*(4, 5)*	0.810	0.995	0.695	0.998	
	8M +LY *vs.* 8M *Notch1*^{cKO}	*(5, 7)*	0.860	0.963	0.598	**0.0077	

Fig. 4. Sustained restoration of canal and otolith function at 8 months by pharmacological inhibition and genetic knockout of *Notch1* in DT-ablated *Pou4f3*$^{DTR/+}$ mice. (A) Schematic of the experimental approach to induce Cre-mediated recombination in *Plp1*^{CreER} *Notch1*$^{fl/fl}$ mice followed by diphtheria toxin (DT) to ablate hair cells. Rotational and translational VORs were recorded 8-month post damage from wild-type (n=4, black), *Pou4f3*$^{DTR/+}$ DT-ablated without treatment (n=3, gray), *Pou4f3*$^{DTR/+}$ DT-ablated +LY (n=5, pink) and *Pou4f3*$^{DTR/+}$ DT-ablated *Notch1*^{cKO} mice (n=7, blue). RVOR gains without visual stimulation **(B)** and with visual stimulation **(C)**. RVOR phases without visual stimulation **(B')** and with visual stimulation **(C').** RVOR distortions without visual stimulation **(B")** and with visual stimulation **(C")**. **(D)** TVOR gains. **(D')** TVOR phases. **(D")** TVOR distortion. All data represent the mean ± SEM. ****$p < 0.0001$, ***$p < 0.001$, **$p < 0.01$ **$p < 0.01$, *$p < 0.05$ by 2-way ANOVA with Tukey's multiple comparisons, reported p-values reported in the graphics are from the comparisons of LY and *Notch1*^{cKO} to the spontaneous regeneration 8 months post ablation. **(E)** Summary table of p-values comparing RVOR and TVOR gains from LY, *Notch1*^{cKO} and wild-type groups.

Inhibition of Notch triggers hair cell regeneration from supporting cells in the newborn cochlea (*34-36*) and in cochlear organoids (*37*), but regeneration is limited in the adult mouse cochlea (*30, 38, 39*). Mammalian vestibular hair cells regenerate spontaneously early in life (*19*), but the extent of the regeneration decreases with age (*11, 12, 24, 33*). We hypothesized that the inhibition of Notch might enhance regeneration in the vestibular system, where chromatin is more permissive than in the cochlea (*40*). The greater functional recovery in the vestibular organs compared to the cochlea was consistent with an inherent capacity to regenerate the mechanosensory receptor cells for balance (*46-48*).

Extensive work on transcription factors and signaling pathways important for hair cell regeneration have led to the use of reprogramming transcription factors, but the extent of regeneration in adults has been limited (*20, 40, 49*). We favored the pharmacological manipulation of the Notch pathway over transcription factor overexpression for reprogramming because inhibition starts a cascade of transcription factor expression that includes Atoh1 as well as downstream transcription factors like Gfi1 and Pou4f3 and also triggers Wnt signaling (*34, 36, 38, 50, 51*). Wnt is important for driving expression of *Atoh1* (*52*), thus acting as a positive signal for regeneration. Notch signaling prevents differentiation by allowing Wnt activity (*34*). Inhibiting Notch signaling also decreases the level of transcription factor, Sox2 (*27, 34, 36, 45, 53-55*). *Sox2* expression is important for hair cell differentiation induced by γ-secretase inhibitor (*34, 50*), with low levels of Sox2 after γ-secretase treatment required to allow differentiation of new hair cells (*36*). We have also found that *Sox2* knockout during early development increases type I hair cells in the vestibular system, while decreasing type II hair cells (*27*), consistent with the finding here that *Notch1* knockout increases the ratio of type I to type II hair cells during regeneration.

The regeneration of mouse vestibular hair cells was achieved in a damage model where 92% of hair cells are ablated. The experiments were performed at 4 weeks of age, when hair cells are mature and there is limited spontaneous regeneration. The recovery of VOR gain seen here in adult mice 2 months after treatment with LY was not observed in damaged but untreated animals, and the regeneration of hair cells was nearly twice that of spontaneous regeneration. The limited regeneration in the absence of drug treatment is consistent with results in adult damage models (*10, 12*) and was limited to type II hair cells (*11, 24, 26*). As compared to previous work with a

GSK3β inhibitor (*45*), which restored only high frequency activity in the utricle and little activity in the semicircular canals, VOR and single unit recording showed that Notch deletion and γ-secretase inhibitor treatment restored both otolith and canal activity across frequencies, consistent with extensive regeneration of both type I and type II vestibular hair cells. The continued improvement in these metrics of vestibular function at 8 months with the γ-secretase inhibitor diverged from the *Notch1*^{cKO}, suggesting that brief inhibition by locally administered drug provided a more stable effect than *Notch1* knockout. This could be explained by the permanent loss of Notch activity in vestibular supporting cells in the *Notch1*^{cKO}, consistent with previous observations that Notch activity is required for the development and maintenance of vestibular organs (*56-58*). It could alternatively be explained by effects on other Plp+ cells, which include vestibular Schwann cells and central nervous system glia (*43*).

The increase in vestibular function with the γ-secretase inhibitor relative to that achieved with a GSK3β inhibitor may provide a route to a better understanding of molecular mechanisms that improve function of hair cells and allow us to correlate type I and II hair cell regeneration to improvement in vestibular function in future studies. The regeneration of hair cells and restoration of vestibular function was based on a clinically relevant metric (VOR). Overcoming the resistance to regeneration is important for clinical progress in the treatment of balance disorders, which are common in older adults (*1, 5*), and treatment with a γ-secretase inhibitor should aid in developing a regenerative therapy to restore vestibular function (*27, 34, 36, 45*).

Acknowledgments
National Institutes of Health grant R01DC020322 (AE)

Author contributions
Conceptualization: AE, HL
Methodology: AE, HL, HZ, WZ
Investigation: AE, HL, HZ, WZ
Visualization: AE, HL, HZ, WZ
Funding acquisition: AE
Project administration: AE
Supervision: AE, HL
Writing – original draft: AE, HL
Writing – review & editing: AE, HL, HW, WZ

Competing interests
AE is a founder and consultant to Audion Therapeutics.

References

1. Y. Agrawal, J. P. Carey, C. C. Della Santina, M. C. Schubert, L. B. Minor, Disorders of balance and vestibular function in US adults: data from the National Health and Nutrition Examination Survey, 2001-2004. *Arch Intern Med* **169**, 938-944 (2009).
2. L. L. Cunningham, A. G. Cheng, E. W. Rubel, Caspase activation in hair cells of the mouse utricle exposed to neomycin. *J Neurosci* **22**, 8532-8540 (2002).
3. R. A. Eatock, K. M. Hurley, Functional development of hair cells. *Curr Top Dev Biol* **57**, 389-448 (2003).
4. R. A. Eatock, J. E. Songer, Vestibular hair cells and afferents: two channels for head motion signals. *Annu Rev Neurosci* **34**, 501-534 (2011).
5. Y. Agrawal, B. K. Ward, L. B. Minor, Vestibular dysfunction: prevalence, impact and need for targeted treatment. *J Vestib Res* **23**, 113-117 (2013).
6. R. Pujol, S. B. Pickett, T. B. Nguyen, J. S. Stone, Large basolateral processes on type II hair cells are novel processing units in mammalian vestibular organs. *J Comp Neurol* **522**, 3141-3159 (2014).
7. R. A. Eatock, J. Xue, R. Kalluri, Ion channels in mammalian vestibular afferents may set regularity of firing. *J Exp Biol* **211**, 1764-1774 (2008).
8. J. M. Goldberg, Afferent diversity and the organization of central vestibular pathways. *Exp Brain Res* **130**, 277-297 (2000).
9. M. A. Mathews, A. J. Camp, A. J. Murray, Reviewing the Role of the Efferent Vestibular System in Motor and Vestibular Circuits. *Front Physiol* **8**, 552 (2017).
10. A. Forge, L. Li, J. T. Corwin, G. Nevill, Ultrastructural evidence for hair cell regeneration in the mammalian inner ear. *Science* **259**, 1616-1619 (1993).
11. J. S. Golub *et al.*, Hair cell replacement in adult mouse utricles after targeted ablation of hair cells with diphtheria toxin. *J Neurosci* **32**, 15093-15105 (2012).
12. K. Kawamoto, M. Izumikawa, L. A. Beyer, G. M. Atkin, Y. Raphael, Spontaneous hair cell regeneration in the mouse utricle following gentamicin ototoxicity. *Hear Res* **247**, 17-26 (2009).
13. E. W. Rubel, L. A. Dew, D. W. Roberson, Mammalian vestibular hair cell regeneration. *Science* **267**, 701-707 (1995).
14. E. W. Rubel, S. A. Furrer, J. S. Stone, A brief history of hair cell regeneration research and speculations on the future. *Hear Res* **297**, 42-51 (2013).
15. M. Scheibinger, D. C. Ellwanger, C. E. Corrales, J. S. Stone, S. Heller, Aminoglycoside Damage and Hair Cell Regeneration in the Chicken Utricle. *J Assoc Res Otolaryngol* **19**, 17-29 (2018).
16. R. M. Walsh, C. M. Hackney, D. N. Furness, Regeneration of the mammalian vestibular sensory epithelium following gentamicin-induced damage. *J Otolaryngol* **29**, 351-360 (2000).

17. J. C. Burns, J. T. Corwin, Responses to cell loss become restricted as the supporting cells in mammalian vestibular organs grow thick junctional actin bands that develop high stability. *J Neurosci* **34**, 1998-2011 (2014).
18. J. C. Burns, B. C. Cox, B. R. Thiede, J. Zuo, J. T. Corwin, In vivo proliferative regeneration of balance hair cells in newborn mice. *J Neurosci* **32**, 6570-6577 (2012).
19. J. C. Burns, J. S. Stone, Development and regeneration of vestibular hair cells in mammals. *Semin Cell Dev Biol* **65**, 96-105 (2017).
20. Z. N. Sayyid, T. Wang, L. Chen, S. M. Jones, A. G. Cheng, Atoh1 Directs Regeneration and Functional Recovery of the Mature Mouse Vestibular System. *Cell Rep* **28**, 312-324 e314 (2019).
21. J. S. Stone, Y. S. Choi, S. M. Woolley, H. Yamashita, E. W. Rubel, Progenitor cell cycling during hair cell regeneration in the vestibular and auditory epithelia of the chick. *J Neurocytol* **28**, 863-876 (1999).
22. J. S. Stone, D. A. Cotanche, Hair cell regeneration in the avian auditory epithelium. *Int J Dev Biol* **51**, 633-647 (2007).
23. T. Wang *et al.*, Uncoordinated maturation of developing and regenerating postnatal mammalian vestibular hair cells. *PLoS Biol* **17**, e3000326 (2019).
24. S. A. Bucks *et al.*, Supporting cells remove and replace sensory receptor hair cells in a balance organ of adult mice. *Elife* **6**, (2017).
25. J. C. Burns, M. C. Kelly, M. Hoa, R. J. Morell, M. W. Kelley, Single-cell RNA-Seq resolves cellular complexity in sensory organs from the neonatal inner ear. *Nat Commun* **6**, 8557 (2015).
26. A. Gonzalez-Garrido *et al.*, The Differentiation Status of Hair Cells That Regenerate Naturally in the Vestibular Inner Ear of the Adult Mouse. *J Neurosci* **41**, 7779-7796 (2021).
27. J. Lu *et al.*, Increased Type I and Decreased Type II Hair Cells after Deletion of Sox2 in the Developing Mouse Utricle. *Neuroscience* **422**, 146-160 (2019).
28. J. S. Stone, R. Pujol, T. B. Nguyen, B. C. Cox, The transcription factor Sox2 is required to maintain the cell type-specific properties and innervation of type II vestibular hair cells in adult mice. *J Neurosci*, (2021).
29. T. Wang *et al.*, Lgr5+ cells regenerate hair cells via proliferation and direct transdifferentiation in damaged neonatal mouse utricle. *Nat Commun* **6**, 6613 (2015).
30. A. A. Iyer *et al.*, Cellular reprogramming with ATOH1, GFI1, and POU4F3 implicate epigenetic changes and cell-cell signaling as obstacles to hair cell regeneration in mature mammals. *Elife* **11**, (2022).
31. K. Kawamoto, S. Ishimoto, R. Minoda, D. E. Brough, Y. Raphael, Math1 gene transfer generates new cochlear hair cells in mature guinea pigs in vivo. *J Neurosci* **23**, 4395-4400 (2003).
32. M. M. McGovern *et al.*, Expression of Atoh1, Gfi1, and Pou4f3 in the mature cochlea reprograms nonsensory cells into hair cells. *Proc Natl Acad Sci U S A* **121**, e2304680121 (2024).

33. R. R. Taylor *et al.*, Regenerating hair cells in vestibular sensory epithelia from humans. *Elife* **7**, (2018).
34. N. F. Bramhall, F. Shi, K. Arnold, K. Hochedlinger, A. S. Edge, Lgr5-positive supporting cells generate new hair cells in the postnatal cochlea. *Stem Cell Reports* **2**, 311-322 (2014).
35. M. W. Kelley, Regulation of cell fate in the sensory epithelia of the inner ear. *Nat Rev Neurosci* **7**, 837-849 (2006).
36. J. S. Kempfle, J. L. Turban, A. S. B. Edge, Sox2 in the differentiation of cochlear progenitor cells. *Scientific Reports* **6**, 23293 (2016).
37. W. J. McLean *et al.*, Clonal Expansion of Lgr5-Positive Cells from Mammalian Cochlea and High-Purity Generation of Sensory Hair Cells. *Cell Rep* **18**, 1917-1929 (2017).
38. K. Mizutari *et al.*, Notch inhibition induces cochlear hair cell regeneration and recovery of hearing after acoustic trauma. *Neuron* **77**, 58-69 (2013).
39. Z. P. Stojanova, T. Kwan, N. Segil, Epigenetic regulation of Atoh1 guides hair cell development in the mammalian cochlea. *Development* **142**, 3529-3536 (2015).
40. H. I. Jen *et al.*, Transcriptomic and epigenetic regulation of hair cell regeneration in the mouse utricle and its potentiation by Atoh1. *Elife* **8**, (2019).
41. M. S. Wolfe, Structure and Function of the gamma-Secretase Complex. *Biochemistry* **58**, 2953-2966 (2019).
42. P. J. Lanford *et al.*, Notch signalling pathway mediates hair cell development in mammalian cochlea. *Nat Genet* **21**, 289-292 (1999).
43. M. E. Gomez-Casati, J. Murtie, B. Taylor, G. Corfas, Cell-specific inducible gene recombination in postnatal inner ear supporting cells and glia. *J Assoc Res Otolaryngol* **11**, 19-26 (2010).
44. S. S. Desai, C. Zeh, A. Lysakowski, Comparative morphology of rodent vestibular periphery. I. Saccular and utricular maculae. *J Neurophysiol* **93**, 251-266 (2005).
45. H. Lahlou, H. Zhu, W. Zhou, A. S. Edge, Pharmacological regeneration of sensory hair cells restores afferent innervation and vestibular function. *J Clin Invest*, (2024).
46. J. T. Corwin, D. A. Cotanche, Regeneration of sensory hair cells after acoustic trauma. *Science* **240**, 1772-1774 (1988).
47. B. M. Ryals, E. W. Rubel, Hair cell regeneration after acoustic trauma in adult Coturnix quail. *Science* **240**, 1774-1776 (1988).
48. A. D. Slowik, O. Bermingham-McDonogh, Hair cell generation by notch inhibition in the adult mammalian cristae. *J Assoc Res Otolaryngol* **14**, 813-828 (2013).
49. Y. Liu *et al.*, Combinatorial Atoh1, Gfi1, Pou4f3, and Six1 gene transfer induces hair cell regeneration in the flat epithelium of mature guinea pigs. *Hear Res* **441**, 108916 (2024).
50. G. Kalra *et al.*, Cochlear organoids reveal transcriptional programs of postnatal hair cell differentiation from supporting cells. *Cell Rep* **42**, 113421 (2023).
51. A. Samarajeewa *et al.*, Transcriptional response to Wnt activation regulates the regenerative capacity of the mammalian cochlea. *Development* **145**, (2018).

52. F. Shi, Y. F. Cheng, X. L. Wang, A. S. Edge, Beta-catenin up-regulates Atoh1 expression in neural progenitor cells by interaction with an Atoh1 3' enhancer. *J Biol Chem* **285**, 392-400 (2010).
53. S. J. Jeon, M. Fujioka, S. C. Kim, A. S. B. Edge, Notch signaling alters sensory or neuronal cell fate specification of inner ear stem cells. *J. Neurosci.* **31**, 8351-8358 (2011).
54. N. Surzenko, T. Crowl, A. Bachleda, L. Langer, L. Pevny, SOX2 maintains the quiescent progenitor cell state of postnatal retinal Muller glia. *Development* **140**, 1445-1456 (2013).
55. M. Wegner, C. C. Stolt, From stem cells to neurons and glia: a Soxist's view of neural development. *Trends Neurosci* **28**, 583-588 (2005).
56. R. M. Brown, 2nd, J. C. Nelson, H. Zhang, A. E. Kiernan, A. K. Groves, Notch-mediated lateral induction is necessary to maintain vestibular prosensory identity during inner ear development. *Dev Biol* **462**, 74-84 (2020).
57. A. Heffer, F. A. Gilels, A. E. Kiernan, Deletion of Notch1 during Cochlear Maturation Leads to Rapid Supporting Cell Death and Profound Deafness. *J Neurosci* **43**, 199-210 (2023).
58. A. Heffer, C. Lee, J. C. Holt, A. E. Kiernan, Notch1 is required to maintain supporting cell identity and vestibular function during maturation of the mammalian balance organs. *bioRxiv*, (2024).
59. Y. Asai *et al.*, Transgenic Tmc2 expression preserves inner ear hair cells and vestibular function in mice lacking Tmc1. *Sci Rep* **8**, 12124 (2018).
60. C. A. Nist-Lund *et al.*, Improved TMC1 gene therapy restores hearing and balance in mice with genetic inner ear disorders. *Nat Commun* **10**, 236 (2019).
61. C. Stewart *et al.*, Effects of high intensity noise on the vestibular system in rats. *Hear Res* **335**, 118-127 (2016).

Materials and Methods

Mice: All mice were obtained from the Jackson Laboratory (Table. S1), housed with open access to food and water. For hair cell loss, *Pou4f3*^{DTR} mice were mated with C57BL/6 mice to obtain *Pou4f3*$^{DTR/+}$ *and Pou4f3*$^{+/+}$(wild-type) mice were used as controls. Only *Pou4f3*$^{DTR/+}$ heterozygous mice were used for hair cell ablation.

For *Notch1* conditional knockout experiments, *Notch1*$^{flox/flox}$ mice were mated with *Plp1*^{CreER} to generate *Notch1*$^{flox/flox}$*;Plp1*^{CreER}. Littermates was crossed with *Pou4f3*$^{DTR/+}$ to get *Pou4f3*$^{DTR/+}$*;Notch1*$^{flox/flox}$*; Plp1*^{CreER}. The homozygous mutants were defined as *Notch1* knockout. Littermates without Cre were used as controls for the spontaneous regeneration. We used *Pou4f3*$^{DTR/+}$*;Notch1*$^{flox/flox}$*; Plp1*^{CreER} crossed *Rosa26*^{tdTomato} (called *tdTomato*) mice for lineage tracing experiments. Male and female mice were used in all experiments. When mated, all progenies were on C57Bl/6J background. Littermates were genotyped with Jackson Laboratory protocols

Sex as a biological variable: In the present studies, mice of both genders were used.

Study approval: All mouse experiments were approved by the Institutional Animal Care and Use Committee of Massachusetts Eye and Ear and the University of Mississippi Medical Center.

Diphtheria toxin administration: Diphtheria toxin (Sigma D0564) was reconstituted in distilled water at 1 mg/ml as a stock solution and stored at -20°C. A working solution was diluted in sterile PBS 1X at 10 µg/ml and freshly prepared prior to each injection. 4-week-old mice received two intramuscular injections of DT at 50 ng/g, spaced 2 days apart. Mice were hydrated with 0.4 ml of lactated Ringer's solution injected subcutaneously at day 0, day 1, and day 2. Food was substituted by high caloric one and hydrogel was provided in the cage.

Tamoxifen injections: For Cre activation, tamoxifen (Sigma T5648) was dissolved in corn oil at 50 mg/ml and administered by intraperitoneal injection to *Pou4f3*$^{DTR/+}$*;Plp1*^{CreER}*;mTmG* mice at P25 for 3 consecutive days prior to DT treatment (2.5 µl/g of tamoxifen solution).

Whole organ culture: Utricles were harvested from 5-week-old mice pretreated with DT, as described above. Utricles of both genders were dissected in cold DMEM/F12 under sterile conditions. After removing the otoconia, utricles were plated in four well petri dishes (1 utricle per well) pre-filled with 90 µl of growth factor-enriched medium, consisting of DMEM/F12 (1:1), N2 (1:100), B27 (1:50) and incubated at 37°C. 1 hour later, medium was replaced and supplemented with either 3 µM CHIR + 1 mM VPA or 0.1% DMSO (controls). Whole organs were maintained in an incubator (37°C, 5% CO2) with medium changes every day, stopped after 2, 5, 10 and 14 days for immunohistochemical analysis.

Round window administration of LY411575: 5-week-old DT-ablated mice of both genders received a unilateral injection of γ-secretase inhibitor (LY411575) onto the round window niche (RW), the contralateral ear was used as a control for the spontaneous regeneration. The drug was diluted in polyethylene glycol 400 (1:2) and artificial perilymph (1:2) to a final concentration of 4 mM. Animals were anesthetized with an intraperitoneal injection of ketamine (100 mg/kg, ip) and xylazine (10 mg/kg, ip). All the surgical procedures were performed in pre-warmed room (26°C), to maintain the body temperature. The fur behind the left ear was shaved with a razor and sterilized with 10% povidone iodine. Under an operating microscope, an incision was made posterior to the pinna near the external meatus. The otic bulla was opened to approach the round window niche. LY411575 solution was injected with a Hamilton syringe and administrated for 2 min. Gelatin was placed on the niche to maintain the solution, and the wound was closed. The solution was administered for 2 min. This approach is widely used clinically and has the advantage of sparing the inner ear but still taking advantage of the local route provided by the round window membrane for delivery of drug into the inner ear (Mikulec et al., 2008). Hydrogel and food gel were placed into the cage daily from the first day after surgery until recovery. Pain was controlled with buprenorphine (0.05 mg/kg) given directly postoperatively and meloxicam (2 mg/kg) injected every 20-24 hours for 3 days. Recovery was closely monitored daily for at least 5 days postoperatively.

Vestibuloocular reflex: Detailed methods were previously described (*59-61*). Briefly, each mouse was implanted with a head holder on the skull. Eye position signals of the left eye were recorded using an eye tracking system (ISCAN ETS-200, ISCAN, Burlington, MA) that was mounted on a servo-controlled rotator/sled (Neurokinetic, Pittsburgh, PA). The eye tracker tracked the pupil center and a reference corneal reflection at a speed of 240 frames per second with a spatial resolution of 0.1 deg. Calibration was achieved by rotating the camera from the left 10 degree to the right 10 degree around the vertical axis of the eye. Following calibration, horizontal head rotations were delivered at 0.2, 0.5, 1, 2 and 4 Hz (60 degree/s peak velocity) to measure the steady state rotational VOR responses. Signals related to eye position and head position were sampled at 1 kHz at 16 bits resolution by a CED Power 1401 system (Cambridge Electronics Devices, Cambridge, UK). Eye movement responses were analyzed using Spike2 (Cambridge Electronics Devices), MatLab (MathWorks, Natick, MA) and SigmaPlot (Systat Software, San Jose, CA). Eye position signals were filtered and differentiated with a band-pass of DC to 50 Hz to obtain eye velocity. Gains and phases of the rotational VORs were calculated by performing a fast Fourier transform on the de-saccaded eye velocity signal and head rotation velocity signal as described (*61*).

Immunohistochemistry: Utricles were harvested and fixed for 30 minutes in 4% paraformaldehyde in PBS, pH 7.4 (Electron Microscopy Services) at room temperature. Unspecific binding was blocked with 10% donkey serum, 0.25% Triton X-100 in PBS for 1 hour at RT. Tissues were incubated overnight at 4°C with specific primary antibodies diluted in

blocking solution (Table S1). Then utricles were rinsed (3X 5 minutes each) in PBS and incubated with the corresponding AlexaFluor secondary antibodies (2 hours at RT) (Table S1), nuclei were counterstained with DAPI (1:1000). Samples were mounted using Prolong Gold antifading (Life Technologies) on glass slides. Positive and negative controls were performed for all immunostaining. The images were acquired with Leica SP8 confocal microscopy and analyzed with Fiji-ImageJ.

Cellular quantification: Cells were counted manually using graphic tools; Cell counter Plugins; of Fiji-ImageJ software. Total hair cell and supporting cell counts per utricle were performed from 20x z-stack images of 29790 μm^2 using a grids method or from the whole sensory epithelium for the newly regenerated hair cells. The count from 29790 μm^2 represents the quantification in fifteen grids (1986 μm^2 each) randomly chosen from both striolar and extrastriolar regions that fell within the sensory epithelium. To get the total cell number per utricle, we computed the area of the sensory epithelium using ImageJ-Measure. We then multiplied the total area by the summed counts from fifteen grids and divided the result by the counted area (29790). Only cells that had a healthy-appearing DAPI-labeled nucleus located in the sensory epithelium were counted as positive.

Statistical analysis: Graph Pad Prism software was used for statistical analysis. All data are presented as means ± SEM and analyzed using Student t-test, one-way ANOVA, or two-way ANOVA. Differences between means were determined by the Mann-Whitney test. Statistical difference was reported for p-values below 0.05; an asterisk indicates significant differences between means ($^{*}p < 0.05$; $^{**}p < 0.01$; $^{***}p < 0.001$; $^{****}p < 0.0001$).